Predicting Overall Survival in Brain Metastasis Patients Using MRI Morphological Features: A Machine Learning and Survival Analysis Approach

Daniela Pomohaci , Emilia-Adriana Marciuc , Bogdan-Ionuț Dobrovăț , Oriana-Maria Onicescu , Sabina-Ioana Chirica , Costin Chirica * , Mihaela-Roxana Popescu * , Danisia Haba

Posted Date: 24 February 2026

doi: 10.20944/preprints202602.1448.v1

Keywords: brain metastasis;overall survival; artificial intelligence; machine learning; MRI data analysis

 doi:10.20944/preprints202602.1448.v1

Article

Predicting Overall Survival in Brain Metastasis Patients Using MRI Morphological Features: A Machine Learning and Survival Analysis Approach

Daniela Pomohaci [1,2], Emilia-Adriana Marciuc [2,3], Bogdan-Ionuț Dobrovăț [2,3], Oriana-Maria Onicescu [4], Sabina-Ioana Chirica [1], Costin Chirica [1,*], Mihaela-Roxana Popescu [2,3,*] and Danisia Haba [2,3]

[1] Doctoral School, Grigore T. Popa University of Medicine and Pharmacy Iasi, 16 Universității Str., 700115 Iasi, Romania
[2] Department of Oral and Maxillofacial Surgery, Faculty of Dental Medicine, Grigore T. Popa University of Medicine and Pharmacy Iasi, 16 Universității Str., 700115 Iasi, Romania
[3] Department of Radiology, Emergency Hospital Professor Doctor Nicolae Oblu, 700309 Iasi, Romania
[4] Faculty of Computer Science, "Alexandru Ioan Cuza" University, 700506 Iasi, Romania
* Correspondence: chiricacostin@gmail.com; drpopescuroxana@yahoo.com

Abstract

Background/Objectives: Our study aims to identify potential new MRI features of brain metastases (BMs) that could be further used in overall survival (OS) assessment. **Methods**: A total of 109 patients with BMs were included. Kaplan-Meier analysis, the log-rank test, and Cox regression were implemented in the survival analysis. Significant features were subsequently incorporated into four distinct machine learning (ML) algorithms to predict six-month survival. **Results**: Survival analysis revealed that multiple brain lesions, synchronous presentation, and restricted diffusion were associated with a poor prognostic value (HR > 1; $p = 0.01$, $p = 0.02$, and $p < 0.005$, respectively). Other features demonstrated a protective effect OS: the absence of extracranial lesions (HR < 1, $p = 0.04$), and the presence of peripheral edema and solid enhancement (HR < 1, $p < 0.0005$). All treatment protocols—including surgery, gamma knife radiosurgery, whole brain radiation therapy, and chemotherapy - showed significantly better survival rates compared to best supportive care (HR < 1, $p < 0.005$). The Neural Networks was the top-performing ML model, achieving an AUC of 0.93. According to the Shapley Additive Explanations analysis, solid enhancement and radiotherapy had a positive impact on OS, whereas a higher number of lesions, larger volumes, and restricted diffusion were associated with negative outcomes. **Conclusions**: Our results confirm that including morphological MRI features of BMs in the prediction of OS significantly contributes to the enhancement of ML algorithms prediction and discriminatory capacity.

Keywords: brain metastasis; overall survival; artificial intelligence; machine learning; MRI data analysis

1. Introduction

Brain metastases (BMs) are one of the most frequent malignant brain lesions in adult patients [1][2]. Intuitively, their detection represents from the start the evolution of a primary tumor, almost exclusively extra-cranial and comes with a poor prognosis, with an overall survival (OS) ≤ 12 months [1][3].

Nowadays, the local treatment of the secondary lesions depends on various factors determined both by the patient's characteristics and the imaging features of BMs [4]. Asymptomatic patients often only benefit from systemic therapies and follow-up, on the contrary, the symptomatic ones are assessed for performance status, intra- and extra-cranial burden of disease [5]. Patients with low

 doi:10.20944/preprints202602.1448.v1

performance status are often treated with non-invasive therapies such as whole brain radiotherapy (WBRT) or palliative and symptomatic therapies. This approach is also preferred in older patients (> 75 years old) were the preservation of the quality of live prevails on cancer therapies as they are known to induce numerous side effects and affect patient's lives.

Therefore, fitter patients are candidates for numerous cancer therapies, both local and systemic. For the patients with unique or solitary BM, the treatment is surgical, followed by adjuvant stereotactic radio-surgery (SRS) or fractionated radiotherapy (SRT) depending on their size [5]. In acute settings of intra-cranial hypertension or acute obstructive hydrocephalus, the debulking of the brain lesions by radical and complete extraction is recommended [4]. Surgical resection remains a viable therapeutic option for multifocal lesions, provided they are situated within non-eloquent cortical or subcortical brain regions [2][4].

Radiotherapy is adopted as a stand-alone treatment in the case of patients with multiple brain secondary lesions [5]. SRS/SRT is preferred to WBRT when comes to fitter patients as it is demonstrated by numerous studies that WBRT does not have always have a role in prolonging OS and SRS/SRT delays the cognitive decline induced by WBRT [4] [6] [7]. Adjuvant SRS/SRT is indicated in different doses in regard to the resected volume [4]. Because adjuvant WBRT minimizes leptomeningeal spread, it is indicated after surgery [2][4].

On the other hand, systemic therapies are different and specific to the primary tumor, they include conventional chemotherapy (CHT), molecular therapy and immunotherapy [5]. Molecular therapies affect cellular mechanisms that sustain and promote tumoral behavior [8]. There is why it is extremely important to know the nature of the primary tumor. In the context of an occult primary malignancy, the administration of targeted anti-tumor therapies remains clinically unfeasible due to the absence of a defined primary site [2]. Novel studies show however, that the tumoral cells of BMs are molecularly different from their primary site. This implies that systemic molecular therapies addressed to the primary tumor could be less efficient in the treatment of their colonies in the brain parenchyma [4].

The follow-up of these patients is more or less standardized, with the use of clinical examinations and at least 1.5 T magnetic resonance imaging (MRI) contrast examinations at 48 hours after surgery and at two-three months intervals [4]. In this case, the MRI protocol should consist of at least pre- and post-contrast T1-weighted (T1W), followed by T2-weighted (T2W) or T2-weighted Fluid Attenuated Inversion Recovery (T2 FLAIR) [9].

Prognostic factors previously used in the appreciation of OS, are: the performance status of the patient, the age of the patient, the primary tumor, the extent of extra-cranial disease, the number and size of BMs, their location and the presence of leptomeningeal disease. The graded prognostic assessment (GPA) score is also used [10] [11]. The disease specific GPA (DS-GPA) is another scale where more prognostic factors are taken into consideration depending on the primary tumor [12] [13]. OS in metastatic brain patient depends on both the intracranial and extracranial containment of the disease [14]. As we can see, these scales have been extensively used as a prognostic evaluation method, without taking the imaging characteristics of the lesions into consideration. Only the dimension and number of lesions are used as imaging criteria in response assessment in neuro-oncology (RANO) and response evaluation criteria in solid tumors (RECIST 1.1) follow-up methods [15]. These criteria are implemented in clinical trials to assess BMs response to different therapeutical strategies [15].

As artificial intelligence (AI) methods and MRI are both continuously evolving, it is safe to ponder that other morphological features could soon be used as imaging follow-up criteria in patients with BMs and other brain tumors [16] [17].

Our primary endpoint is to contribute to this process and evaluate the prognostic value of morphological conventional and functional MRI features of metastatic brain lesions in connection with the clinical characteristics of BMs patients and their treatment.

2. Materials and Methods

We retrospectively analyzed patients that were diagnosed and treated for BMs in our hospital from 2019 to 2023. Our study has a single centered observational nature.

 doi:10.20944/preprints202602.1448.v1

2.1. Patients' Inclusion and Exclusion Criteria

In total 540 cases were analyzed. Patients underwent careful selection after predefined inclusion and exclusion criteria. Inclusion criteria are:

1. age > 18 years old;
2. patients diagnosed and histopathological confirmed with brain metastases;
3. patients that underwent at least one initial IRM with contrast, before any treatment;
4. Initial MRI protocols consisting of T1W, T2W, T2 FLAIR, susceptibility weighted imaging (SWI), diffusion-weighted imaging /apparent diffusion coefficient map (DWI/ADC) and contrast enhanced T1W (CE T1W).

Exclusion criteria are:

5. patients younger than 18 years old;
6. patients with post-operative MRI of single BM as initial imaging data;
7. patients that lacked MRI investigations;
8. incomplete MRI investigations.

After applying the selection criteria, a final number of 109 patients were included in this study. We then followed their evolution for a period of minimum one month to a maximum of 52.1 months, our end data being 06/16/2024. The survival time was calculated from the histopathological diagnosis of BM till the death date or end of follow-up period of the study.

2.2. The MRI Protocol

In order to examine BMs features we used a Signa Explorer General Electric Medical Systems MRI machine with a field strength of 1.5 Tesla. With the aim of obtaining maximum information on MRI characteristics, we included sequences such as T1W, CE T1W, T2W, T2W FLAIR, essential for the diagnosis of BMs [4], as well as SW and DWI/ADC. These sequences are extremely useful in visualizing tumoral behavior, as "blooming" on SWI represents hemorrhage or vascular signal, detecting the hemoglobin inside the blood vessels or in the perivascular space, and high DWI signal with low ADC map values corresponds to high cellular count [18]. As indicated by the EANO-ESMO guidelines we included 3D post-contrast T1W, acquired at a delay of several minutes [4]. The MRI acquisition parameters are listed in Table A.1 in the Appendix A1 section.

2.3. Data Collection

We extracted two different sets of data: data at the beginning of the study regarding the patients' status and metastatic burden, and follow-up data represented by the treatment, post-treatment evolution and OS.

Regarding post-treatment evolution we included post-surgical or radiosurgery complications like distant brain failure after SRS/SRT, local recurrence after surgery or histological confirmed radio-necrosis after radiotherapy. Other complications taken into consideration were infections or strokes.

The therapeutical options that have been used are: surgical resection, radiosurgery, WBRT, in fewer cases CHT and best supportive care (BSC).

To describe the metastatic lesions, we analyzed MRI features as volume, peripheric edema, the presence of central necrosis or cystic components, restricted diffusion, internal hemorrhage and localization.

We assessed every single brain lesion from every patient. For example, if a patient had only one BM at diagnosis, we only described its characteristics. Conversely, if the patient had multiple lesions, we introduced the features of every secondary lesion present at diagnosis in our database.

The lesions were grouped by the greater diameter value in BMs less than 5 mm, between 5 and 10 mm and equal to or above 10 mm. We estimated the volume of every lesion using the ellipsoidal method [19].

This approach is similar to RANO-BM or RECIST 1.1 criteria where lesions are separated in measurable (diameter greater than or equal to 10 mm) and non-measurable (diameter lesser than 10 mm) [20]. The difference is that we calculated the volume of both measurable and non-measurable BMs, as usually only measurable lesions are further estimated in follow-up MRI investigation, while the non-measurable ones are noted in presence or absence and number [20].

 doi:10.20944/preprints202602.1448.v1

2.4. Statistical Analysis

We organized a dedicated database in Excel in order to categorize patient data across three primary domains: clinical characteristics, MRI-based morphological features, and treatment protocols.

We separately analyzed prognostic factors that depend on the patient characteristics (age, sex, comorbidities – diabetes, smoking status, presence of extra-cranial metastases, synchronism of BM and primary tumor diagnosis, leptomeningeal metastases, complications); the imaging features of the secondary brain parenchymal lesions (location, type of lesion – solid (with/ without central necrosis), cystic or mixed, the presence of diffusion restriction, intralesional hemorrhage and peritumoral edema.

The volume, the number of the BMs, the primary tumors' nature and treatment options (including gamma-knife (GK), surgery, WBRT, CHT and BSC) are additional variables that were examined and consequently included in the final algorithm.

We generated the explanatory data analysis (EDA) for the categorical and numerical variable [21].

We then used the Kaplan-Meier (KM) method to obtain the survival curve for every attribute and the log-rank test to appreciate the difference in survival between groups [22][23].

The univariate Cox proportional hazard was furtherly applied for all the significant variables in the univariate survival analysis, calculating the p-value, the hazard ratio (HR) and the intervals of confidence (CI) [24]. Multivariate Cox regression analysis was also useful in order to compare survival rates between groups with similar covariates (treatment, contrast intake type and volume) [24].

For every test, we considered statistically significant a p-value lesser or equal to 0.05. Log-log plots of the Cox Regression tests were also generated in order to visually verify the HR assumptions [24].

2.5. AI Algorithms

Four machine learning (ML) algorithms were implemented in evaluating the prediction of survival at 6 months (selected as threshold value) from the time of diagnosis. These models were developed using only processed data, in three different setups: first using only patient data, secondly including only MRI features and finally the third, assessing both sets of data together.

We trained every algorithm selecting 80% of our real-world data and internally validated them on the rest of 20% of data. The training data was obtained mainly from patients diagnosed in the first four years (2019-2023), with a total of 87 patients, the rest of 22 patients, diagnosed in the year 2023-2024 represents the validation dataset. This method of validation is also known as temporal validation and lies in between internal and external validation, as new internal data is used [25].

The four machine learning algorithms implemented are:

- The extreme Gradient Boosting (XGBoost) is a machine learning algorithm particularly well-suited for imbalanced datasets, as it can handle classes with significantly different frequencies and provide accurate predictions despite the imbalance [26];
- Neural Network (NN) is a machine learning algorithm that uses mathematical representations of neurons (being built similarly to how human brain neurons work) suited for complex feature interactions [27] [28][29];
- K-nearest neighbor (KNN) is a classification or regression ML model that predicts the value of data based on the average value calculated from a number of *k* nearby data points (neighbors) [30];
- Random forest (RF) a largely applied machine learning model that uses multiple decision trees, considered suitable for heterogeneous datasets due to lower overfit predisposition in small data sets [31] [32].

2.6. Model and Feature Importance Assessment

We compared the classification power of the four different AI prediction models after their training and internal validation by calculating specific metrics [33][34]:

 doi:10.20944/preprints202602.1448.v1

- Accuracy – the capacity of the model to estimate the true positives and true negatives from the total of true and false negatives and positives;
- Precision – the capability to identify the true positives from the total positives results;
- Specificity – identification of the true negatives from the false positives results and true negatives;
- Recall or sensitivity – demonstrates the model sensitivity to detecting true positives from false negatives and true positives;
- F1-score – is the harmonic mean between sensitivity (recall) and precision;
- The time-dependent receiver operating characteristics (ROC) and the aria under the ROC curve (AUC) summarize the discriminatory capability of the model.

We implemented the Shapley Additive exPlanations (SHAP) method for every model in the complete data-set (clinical + treatment + MRI morphological data) to attain feature importance [35]. SHAP assesses the degree of contribution of every attribute, by also representing if the variable has a positive or negative effect on the prediction models, thus making it easier to interpret from a clinical point of view [35].

2.7. Processing Environment

Python (version 3.13.5) was utilized in order to perform the statistical analysis. The Python packages used were: 'pandas', 'keras', 'scikit-learn', 'xgboost', 'shap' and 'matplotlib'.

3. Results

3.1. Patients' Characteristics

Our cohort consisted of a total of 109 patients, 38 (34.9%) women and 71 (65.1%) men, with ages ranging from 21 to 83 years old with a median age of 73 years old.

At the end time of monitoring, 21 of 109 (19.3%) patients were still alive.

The characteristics of the patients included in this study and their implication in OS are listed in Tables A2 and A3 found in the Appendix A section.

The importance of every variable in survival analysis has been estimated using the log-rank test, the KM curves of the ones that were significant (log-rank p-value ≤ 0.05) are visible in Figure 1. Consequently, by applying the univariate Cox proportional hazard model, we calculated the HR, p-value and CI (Table 1).

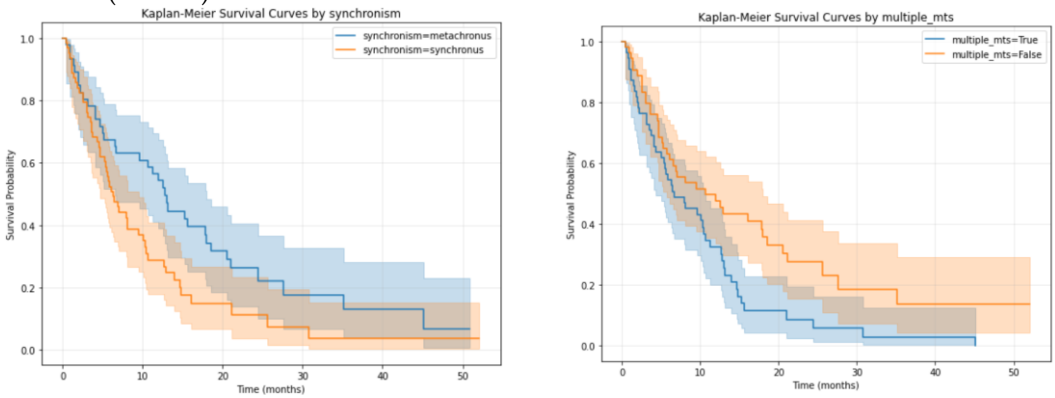

(**a**) (**b**)

 doi:10.20944/preprints202602.1448.v1

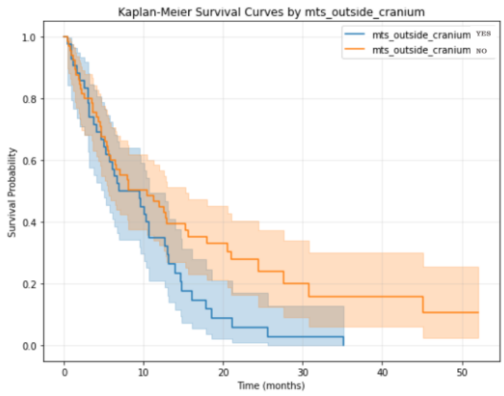

(c)

Figure 1. KM survival curves for clinical data: (**a**)metachronous vs synchronous BMs, p-value of 0.02; (**b**)single vs multiple BMs, p-value of 0.01; (**c**) presence of extracranial metastases, p-value of 0.04.

The time of BMs diagnosis in relation to the diagnosis of the primary tumors had an important implication in survival (p=0.02 – log-rank, Figure 1.a). Patients with synchronous diagnosis or diagnosis of both BMs and primary tumor at the same time, had a poorer prognosis compared to the patients with a metachronous diagnosis (patient who were already diagnosed with different primary tumors and had been monitored and treated).

By implementing Cox regression analysis for the synchronous group, we obtained a p-value of 0.02, HR = 1.68 and CI (1.09-2.60) suggesting a higher risk (68%) of death, compared to the metachronous group. In our cohort, the majority of patients were diagnosed with stage IV tumoral disease with BMs (synchronous - 63 patients (57.8%) and 46 (42.2%) were already known with primary tumors, developing BMs later in the evolution of the disease (metachronous).

Table 1. Univariate Cox Regression results for clinical data.

Data	HR	CI (-95%)	CI (95%)	p-value
Metachronous (42.2%)	Reference	Reference	Reference	Reference
Synchronous (57.8%)	1.68	1.09	2.60	0.02
Single metastasis (49.54%)	Reference	Reference	Reference	Reference
Multiple metastases (50.46%)	1.73	1.13	2.66	0.01
EM* (38.53%)	Reference	Reference	Reference	Reference
No EM* (61.47%)	0.63	0.41	0.97	0.04

*Extracranial metastases.

The number of secondary lesions for patient varied from 1 (single BM) to 30, with a median number of 2. The number of patients with single BM was 54 (49.54%) and had a greater rate of survival compared to the 55 (50.46%) patients who had been diagnosed with multiple secondary brain lesions (p=0.01 by both log-rank and Cox regression, with HR=1.73, CI=1.13-2.66).

The presence of other systemic metastasis at diagnosis has been proved to be important in our data-set, as there was a significant difference in survival (p=0.03 – log-rank, p=0.04, HR =0.63, CI (0.41-0.97) - Cox regression) with the longest survival time being of 52 months for patients without systemic tumoral spread compared to 32 months for the other group.

No difference has been found in survival time using the log-rank method regarding the age of the patients (less than 65 years old compared to more than 65 years old, p-value of 0.4), the sex of the patients (p=0.1), the type of primary tumor, the presence of diabetes (p=0.47), the smoker status (p=0.41), leptomeningeal involvement (p=0.98) or other post-treatment local complications (p=0.59).

3.2. Metastatic MRI Features

 doi:10.20944/preprints202602.1448.v1

In total we analyzed the MRI morphology of 370 secondary brain lesions from the 109 patients included in the study. The characteristics of the secondary brain lesions are listed in Table A4 in the Appendix A section along with the EDA for OS.

The importance of the morphological MRI features in survival analysis has been estimated with the log-rank test (Figure 2). Using the univariate and multivariate Cox proportional hazard method, we calculated the importance in the prediction of OS for every variable (Table 2).

The presence of internal vascularization has a statistically significant effect on the survival prognosis, with a p-value of 0.03 -log-rank, p=0.01, HR=0.72 (CI =0.56 to 0.94) in the Cox regression model.

Because the two KM curves comparing the non-vascular group (94 metastases – 25.4%) and the neovascularized one (276 lesions – 74.6%) cross at 20 months and again after 35 months of follow-up, interpreting these results can be challenging. Neovascularization can be seen as a protective factor (HR<1), as the probability of being alive is higher in the neovascularized lesions group than in the other one.

Another surprising result was the p-value <0.005 (log-rank), p=0.0006, HR=0.59 (CI=0.44-0.8) Cox Regression, for internal bleeding, suggesting tumoral hemorrhage in small quantities (we mostly observed microbleeds lesions in the tumoral tissue) might be associated with better outcomes.

The 68 (18.38%) lesions with internal hemorrhage showed better survival rates at any time compared with the other 302 metastatic tumors (81.62%) (see Figure 2b).

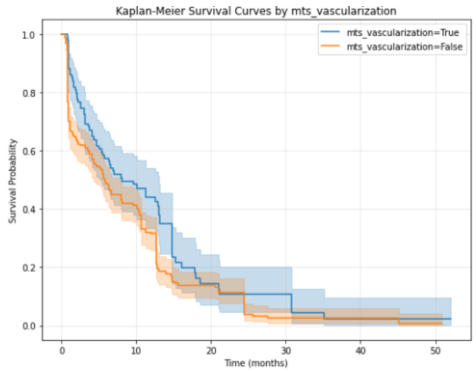

(a)

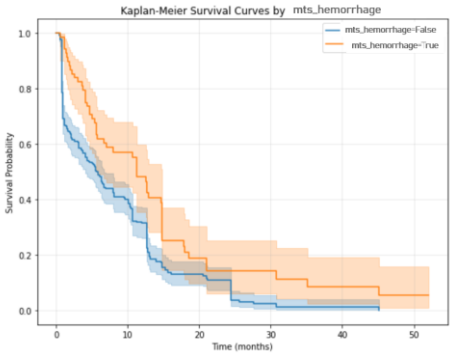

(b)

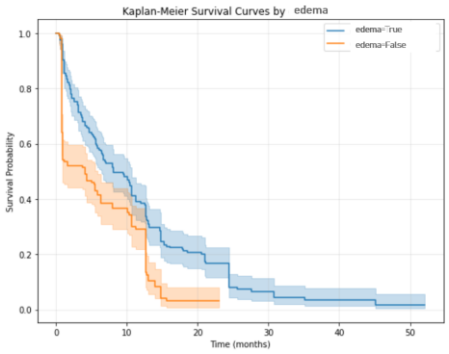

(c)

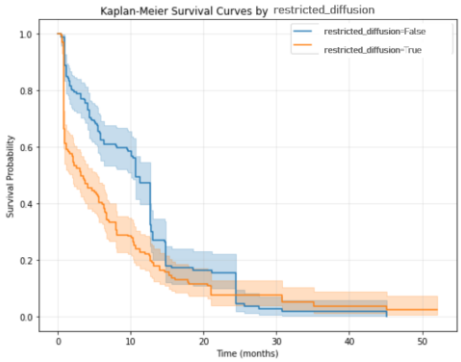

(d)

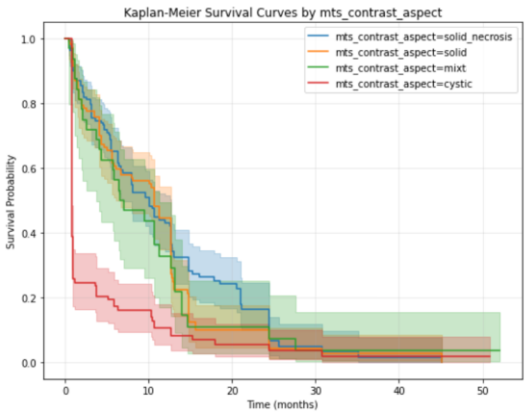

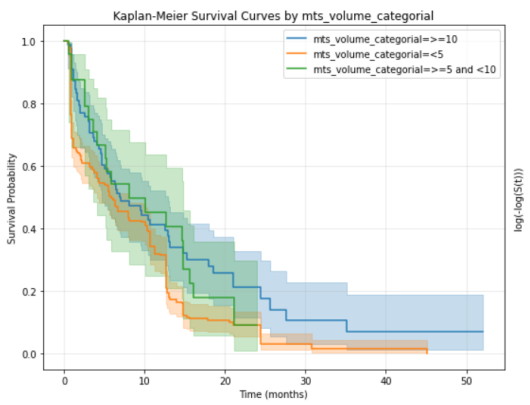

 doi:10.20944/preprints202602.1448.v1

(e) **(f)**

Figure 2. KM survival curves for MRI features and log-rank p-values: (**a**) presence of internal neo-vascularization, p-value of 0.03; (**b**) presence of internal bleeding, p-value <0.005; (**c**) presence of peripheric edema, p-value <0.005; (**d**) presence of restricted diffusion of tumor, p-value <0.005; (**e**) contrast intake (multivariate Cox Regression – see p-values in Table 5); (**f**) metastatic diameter (multivariate Cox Regression see p-values in Table 2).

The presence of peripheric edema is also associated with a better prognosis compared to the group that showed no edema, with a p-value <0.005 (log-rank), $p=0.01x10^{-5}$, HR=0.53 (CI=0.42 - 0.67) Cox regression.

Restricted diffusion is associated, in case of malignant tumors, with a great cellular count suggesting a dense neoplastic tissue. Our results strongly suggest that cellularity is correlated with a lesser probability of survival (p<0.005 - log-rank, $p=0.03x10^{-3}$, HR=1.59, CI=1.27-1.98 – Cox regression).

For the first 25 months (1 year and 1 month), diffusion restriction lesions had a worse prognosis compared to less dense metastases. But, surprisingly, after the 25 months the curves overlap and interchange, suggesting that later in their evolution, BMs have a similar prognosis, independent of cellularity.

The implications of these results are further explained in the Discussion section.

Table 2. Univariate and multivariate Cox Regression results for MRI features.

Feature	HR	CI (-95%)	CI (95%)	p-value
No vascularization (74.6%)	Reference	Reference	Reference	Reference
Vascularization (25.6%)	0.72	0.56	0.94	0.01
No hemorrhage (81.62%)	Reference	Reference	Reference	Reference
Hemorrhage (18.28%)	0.59	0.44	0.8	0.0006
No edema (43.51%)	Reference	Reference	Reference	Reference
Edema (56.48%)	0.53	0.42	0.67	$1x10^{-7}$
No diffusion (48.38%)	Reference	Reference	Reference	Reference
Diffusion (51.62%)	1.59	1.27	1.98	$3x10^{-5}$
Cystic (25.2%)	Reference	Reference	Reference	Reference
Mixt (8.6%)	0.39	0.26	0.6	$1x10^{-5}$
Solid (28.9%)	0.37	0.27	0.5	$7x10^{-11}$
Solid with necrosis (37.3%)	0.33	0.25	0.44	$2x10^{-14}$
Diameter <5 (72.5%)	Reference	Reference	Reference	Reference
>=5 and <10 (6.5%)	0.81	0.44	1.11	0.1
>=10 (21%)	0.7	0.47	0.84	$1x10^{-3}$

The contrast intake type was also assessed, and the lesion were classified into solid, with (138 – 37.3%) or without central necrosis (107 – 37.3%), cystic (93 – 25.2%) or mixed lesions (32 -8.6%); cystic lesions had the worst prognosis compared to the other three types: every other contrast intake type had a HR<1 in the first 25 months, with a lower risk of premature death (Table 2), thus a better survival rate (Figure 2.e).

Regarding the lesions' dimensions, the majority of BMs (268 in total) had the maximum diameter lesser than 5 mm (72.5%), only 78 (21%) having diameters greater than or equal to 10 mm.

A significant difference was found between the three groups, with better survival rate for lesions with a diameter equal or greater than 10 mm (p=0.001, HR=0.70, CI=0.47-0.84 – multivariate Cox regression – Table 2).

Table A5 and A6 in the Appendix A section, show the number, diameters (mm) and volumes (cm^3) of the BMs.

Additional morphological features, including anatomical localization (supratentorial vs. infratentorial) and hemispheric laterality (left vs. right), did not reach statistical significance.

3.3. Treatment Options

 doi:10.20944/preprints202602.1448.v1

Regarding the treatment options, they varied due to changes in therapy protocols and availability at our hospital. Patients diagnosed from 2019 to 2022 were mainly surgically treated (99 patients in total – 90.8%); beginning with the year 2022, the majority of the patients has been also treated with gamma knife (GK) SRT (22 patients – 20.2%).

Table A7 (in the Appendix A section) depicts the number of patients treated with the different methods and their OS time in months.

To summarize, 22 of the cases that were surgically treated (99/109), also received GK therapy. The SRS/SRT protocols differed as follows:

- 10 received adjuvant SRT;
- other 5 patients previously underwent adjuvant WBRT (here SRT was used as secondary treatment after relapse);
- in 3 cases, GK was performed before and after the surgery;
- 4 cases where only neoadjuvant GK was performed, with the administration of one radiotherapy session one day before surgery.

The most used adjuvant SRT protocol consisted of the administration of 30 Gy in three different fractions of 10 Gy at an interval of two weeks, beginning 1 mouth after surgical intervention.

Of the rest of WBRT treated patients, 3 underwent radiotherapy after the surgical resection and only one 1 was treated by WBRT alone. In total 9 patients were treated with WBRT. CHT was an option for only 13 patients, that benefitted from other therapies as well. Only 6 patients were followed with BSC and symptomatic therapy management.

The importance of treatment choice in survival analysis has been estimated using the log-rank test (Figure 3). Consequently, the univariate and multivariate Cox Regression results for every treatment option can be observed in Table 3.

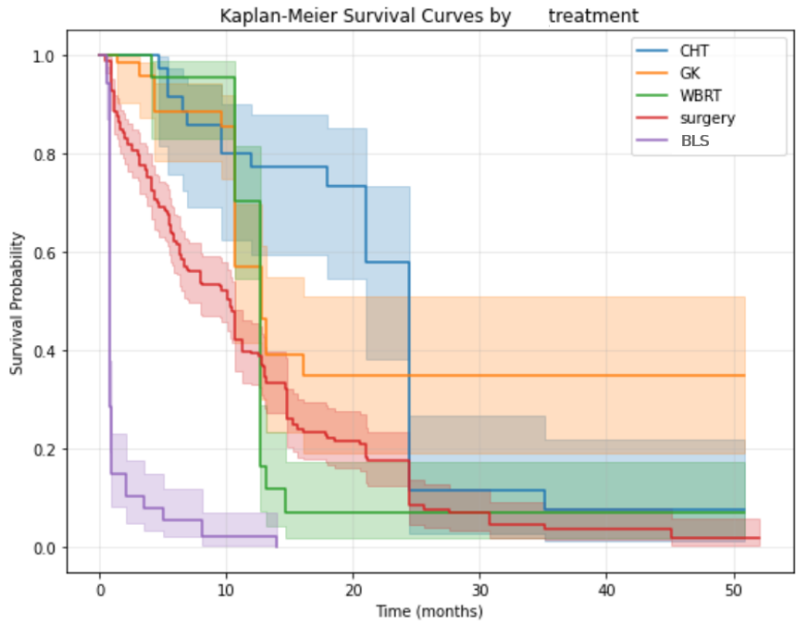

Figure 3. KM survival curves for treatment options compared to BSC and log-rank p-values: CHT p-value of 0.05; surgery p-value of 0.01; GK p-value <0.005; WBRT p-value of 0.03.

Every treatment choice is significant in improving OS in BMs patients, as shown in Figure 3, with a p-value calculated with log-rank test of 0.05 for CHT, 0.01 for surgery, 0.03 for WBRT and a p-value < 0.005 for GK.

Both in the univariate and multivariate Cox regression analysis (exception CHT with univariate p-value of 0.055), every treatment option reached a better prognosis compared to BSC only, with HR<1 and significant p-values (<0.05).

 doi:10.20944/preprints202602.1448.v1

In Figure 3 we can see that the WBRT KM survival curve is the first one to have similar OS appreciation values as BSC after just 14 months; following are surgery and CHT at approximatively 24 months.

Of the four treatment types, GK maintains a survival probability of 35% for over 50 months, longer than the other groups. In this group, we had different therapeutical strategies that were tailored to specific situations, even so, the SRS/SRT patients had the best survival rate indifferent of the timing of radiation, compared to surgery alone.

Table 3. Univariate and multivariate Cox Regression results for treatment options.

Treatment	Univariate				Multivariate			
	HR	CI (-95%)	CI (95%)	p-value	HR	CI (-95%)	CI (95%)	p-value
BSC (6)	Reference	Reference	Reference	Reference	Reference	Reference	Reference	Reference
CHT (13)	0.52	0.27	1.02	0.055	0.37	0.24	0.57	$4x10^{-6}$
Surgery (99)	0.4	0.2	0.78	0.01	0.2	0.32	0.73	$5x10^{-26}$
SRT (GK) (22)	0.31	0.16	0.63	<0.005	0.48	0.16	0.36	$5x10^{-4}$
WBRT (9)	0.37	0.15	0.91	0.03	0.25	0.15	0.27	$3x10^{-12}$

3.4. Prediction Performance of AI Models

For the training of the four ML models, we used 80% of our data, selecting the patients from 2019 till the end of 2023 (87 patients total – 79.8%). For the temporary validation, the rest of 22 patients (20.2%) diagnosed from 2023 to 2024 have been used as new data.

We chose the features that were significant in the survival analysis effectuated with log-rank and Cox Regression and used them in the model creation as well.

For the clinical dataset we used these variables: 'synchronism', the number of lesions, the presence of systemic secondary lesions and the treatment ('CHT', 'surgery', 'WBRT', 'GK' and 'BSC'). The MRI morphological dataset was composed by the presence of 'vascularization', 'hemorrhage', 'peripheric edema', 'restricted diffusion', the type of contrast intake and the volume of lesions expressed in cm^3. Regarding number and volume of lesions we opted to include numerical values as opposed to categorial ones, in order to appreciate the continuity of the data and its effect on survival.

We analyzed the performance parameters of the prediction models, first by only including clinical data (Figure B.1 found in Appendix B), secondly with only MRI morphological data (Figure B.2 found in Appendix B) and, finally both sets of data at once, visible in the heatmap Figure B.3 found in Appendix B.

With regard to the clinical data (Figure B.1), the models performed the poorest with low accuracy (54% for XGBoost, 54% for RF, 50% - KNN and 36% NN), very low specificity (16% XGBoost, 33% RF, 16% - KNN and 33% for NN); slightly better precision (68% XGBoost, 71% RF, 66% KNN and 60% NN); low sensitivity (recall) (68% XGBoost, 62% RF, 62% KNN and 37% NN), low F1-score (68% XGBoost, 66% RF, 64% KNN and 46% NN), and poor AUC (0.54 XGBoost, 0.54 RF, 0.45 KNN and 0.30 NN). The overall best model in this scenario was XGBoost, but itself with poor discrimination power and very low specificity.

In the MRI features dataset (Figure B.2), the models performed similarly to the first case. RF was the best prediction model with low accuracy (75%), moderate specificity (83%); poor precision (69%), recall (61%), F1-score (65%) and AUC of 0.73. The other models obtained lower values, except for sensitivity (recall) with a value of 77% for the XGBoost model and of 91% for the NN model.

After training the ML models on both sets of data, we obtained different results regarding the models' classification power, the AUC values achieved by every program are presented in Figure 4.

Models that displayed greater accuracy than the Random Classifier are NN and XGBoost with an excellent discriminatory power (AUC) of 0.93 and respectively 0.90. The other two models, KNN and RF had a poor discriminatory power with an AUC of 0.61, respectively 0.58.

 doi:10.20944/preprints202602.1448.v1

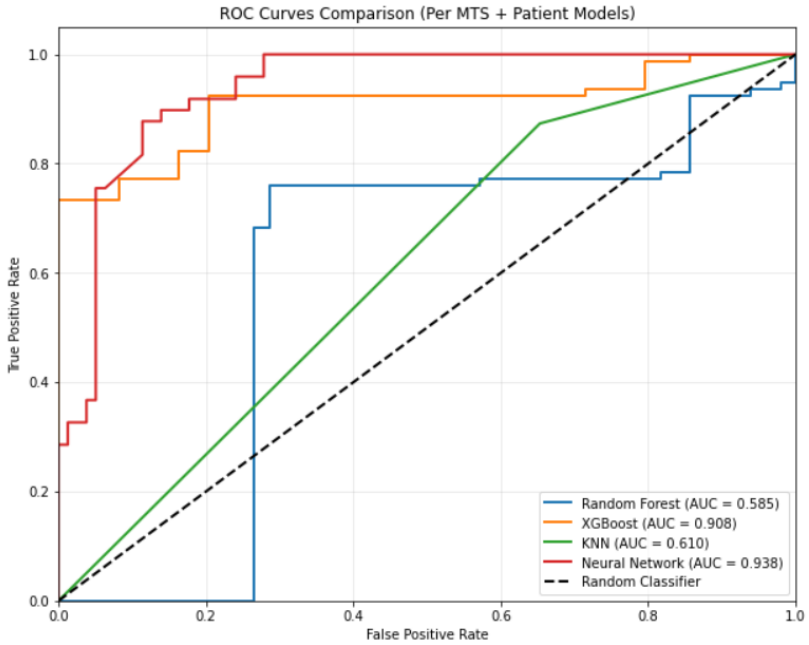

Figure 4. AUC for every model after training on both clinical and morphological data.

In Figure B3 from Appendix B, the other metrics are also displayed.

NN proved to be the most performant model of the four, with an accuracy of 86%, precision of 82%, specificity of 88%, recall of 83%, F1-score of 82% and an AUC of 0.93 (with excellent discrimination).

XGBoost follows the NN model with an accuracy of 68%, precision of 67%, specificity of 28%, recall of 92%, F1-score of 78% and an AUC of 0.90. KNN was the model that obtained the next best results, with an accuracy of 67%, precision of 68%, specificity of 34%, recall of 87%, F1-score of 76% and an AUC of 0.61 with lower discrimination.

The least performant model was RF, displaying the lowest metrics: accuracy of 63%, precision of 68%, specificity of 42%, recall of 75%, F1-score of 71% and an AUC of 0.58 with poor discrimination.

3.5. Model Interpretability

With the aim of identifying the most important features and their implication on survival, we implemented SHAP for every model. As NN was the most performant one in the last case (all variables included) we opted to show the feature importance in BMs survival prediction for the NN model (Figure 4).

As it is shown in the SHAP heatmap, the volume of the lesions has the greatest impact on survival as follows: greater volumes are associated with poor prognosis. The number of lesions is also associated with a negative impact on survival, as numerous BMs mostly correspond to negative values on the impact ax; with a cluster of patients of numerous lesions associated with positive impact (seen in Figure 4 as numerous bright pink dots).

Another morphological feature associated with greater overall-survival is the presence of a solid portion of the lesions that has contrast intake (pink dots); in opposition to cystic or mixed lesions (blue dots) that are associated with poor survival.

Other MRI features found to be valuable in the model prediction are the presence of internal vascularization and restricted diffusion that are associated with a poor prognosis, and hemorrhage that seems to be more of a good prognosis factor.

 doi:10.20944/preprints202602.1448.v1

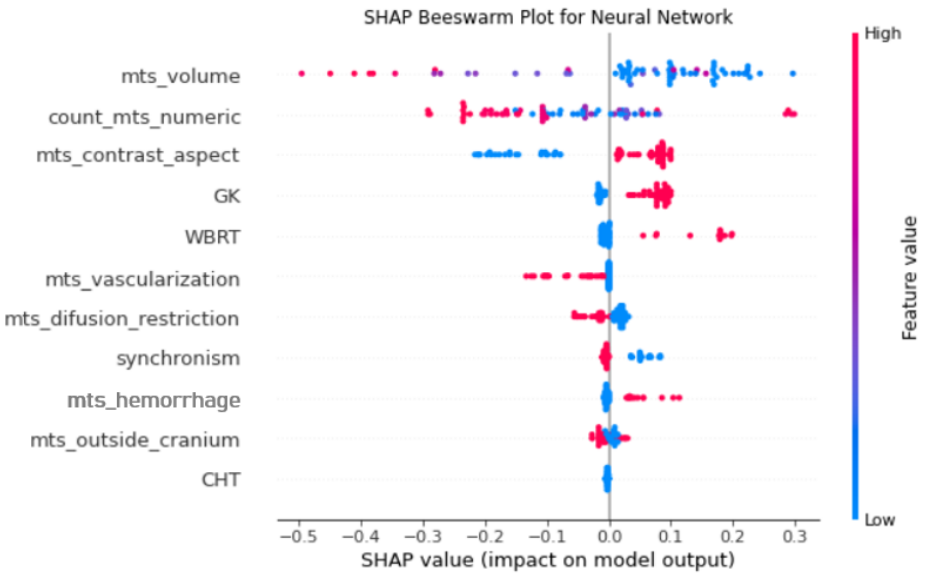

Figure 5. SHAP showing feature relevance using clinical and MRI morphological data for the NN model.

Even though the presence of extracerebral metastases and the synchronous had been selected by SHAP in the NN model, their implication in survival prediction is low, as both are really close to the zero value on the impact ax.

Concerning treatment methods, WBRT and GK are greatly associated with positive values, having thus, a positive impact on the prediction model.

4. Discussion

4.1. Log-Rank and Cox Regression Results' Implications

Regarding clinical characteristics, only a limited number of variables emerged as significant prognostic indicators for survival: the presence of extracerebral metastases, the synchronous presentation and multiple brain lesions. The high number of BMs and the presence of extracerebral metastases are poor prognostic factors that are already used in different clinical sets, being included in prognostic tools assessment, like GPA [12].

The chronological interval between the primary tumor diagnosis and the detection of brain involvement was identified as a critical determinant of OS.

In the case of synchronic diagnosis of the primary tumor and the BMs, the local development and systemic spread of cancer have already taken place as involvement of brain parenchyma occurs later in extracranial neoplasia. While in the case of a metachronous diagnosis of BMS, the patient is known with a primary tumor, treated and in certain cases even screened for the onset of BM, benefitting the patients and ensuring a longer OS [1]. Other studies reached similar conclusions and sustain that time of diagnosis might be an important prognosis factor [6]. However, synchronous diagnosis should not be the reason to avoid performing a surgical resection of BM, as Potthoff et al. found that there was no difference in survival after surgical removal between the two groups [36].

Although the nature of the primary tumors has been assessed, none was specifically more aggressive than others in our cohort of patients. Only melanoma metastases showed a poor but not significative effect on OS (p=0.07, log-rank). Melanoma patients had the shorter OS, with a median survival of 4 months, in agreement to other findings [1].

Including the MRI features gave our work more robustness in OS appreciation. Nonetheless, the focus over the MRI aspects of every secondary lesion of every patient is a novel approach, as the majority of the studies priorly conducted used clinical data only [6].

Of the variables that we included, the peripheric edema, the presence of internal hemorrhage and vascularization, diffusion restriction, the type of contrast intake and the volume were the most important features.

 doi:10.20944/preprints202602.1448.v1

The presence of vascularization and hemorrhage could be the result of a visible blood-brain barrier rupture (microhemorrhages) that ensured a better response to local or systemic treatment. Another theory could be that blooming on SWI has been wrongly assessed as of vascular nature instead of calcification. This could be avoided by introducing a native computer tomography examination of the same patients, priory to treatment, as the values in Hounsfield units for calcification are considerably higher than the ones suggesting hemorrhage [37]. Finally, another plausible reason could be the existence of some king of interrelation between different variables that can alter the results.

As formerly stated, the presence of restricted diffusion in any brain tumor is associated with worse outcomes; by its nature high tumoral cellularity is linked with an aggressive behavior and poor OS [38]. As an extent, restricted diffusion in BMs is considered a poor prognosis factor. Our results confirm the presence of restricted diffusion being associated with a worse prognosis ($p<0.005$ log-rank and Cox Regression).

Regarding the tumoral edema, edematous BMs have a better prognosis, mostly because edema suggests the presence of the lesion, even if its diameter in lesser than 5 mm, thus making it visible. Edematous lesions may also have a slower growth rate, slowly compressing the adjacent brain parenchyma without invasion. The presence of edema may also cause nonspecific symptoms like intracranial hypertension, rushing the imaging detection of the tumors and consequently early treatment.

An additional feature of growing clinical interest is the difference between perilesional edema and tumoral brain invasion, as the latter corresponds to aggressive tumors like glioblastoma [39]. In this case restricted diffusion and diffusion tensor imaging could make a difference by the early identification of brain parenchyma invasion and consequently being able to opt for a more appropriate treatment [39] [40]. In regard to BMs, this differentiation is yet to be pursued, as they are less prone to invade the adjacent brain parenchyma than the aggressive primary tumors [38]. Although diffuse infiltration may also be seen in more aggressive BMs [41].

Compared to the other contrast intake types, the cystic lesions had the poorer prognosis, suggesting that treatment protocols that are commonly used in BMs are less suitable for this type of lesion. Cystic lesions are also known to be more resistant to radiotherapy [2]. This resides in the fact that in a fluid-filled lesion, SRT can only be effective on the walls of the lesion as the cyst can contain cellular debrides and other residues, but not viable tumoral cells. In one study that assessed morphological MRI and volumetric data, the thickness of the rim was predictive of better progression-free survival [14].

Regarding the number of secondary brain lesions and their volumes, we can safely sustain that there is an inversely proportional relation between them in our cohort: a patient with numerous lesions, also has smaller lesions and a patient with fewer BMs features greater lesions (see Tables A5 and A6 in the Appendix A).

We found that single lesions have better OS and thus lesions with greater diameters obtained better OS as well in the survival analysis. A reason could be that surgical removal of BM before SRT in single lesion or oligometastatic disease (less than 5 lesions), is a protective factor even in bigger lesions (>2 cm diameter) compared to SRT alone [42]. In our case, all the patients that benefitted from GK (22/109) were also surgically treated. These patients were the ones with a single lesion (10/22) or oligometastatic disease (8/22); other 4 patients had a number of lesions greater than or equal to 5, but lesser than 10.

The survival analysis was useful in order to identify the best treatment choices from the ones that have been used. This was possible by comparing the OS in different treatment groups. Results strongly suggest that every treatment provides better OS than BSC. The one that showed a steady protective HR value over time (after 25 months) was GK.

This approach seems to be the best one in the case of single or oligometastatic disease: surgery and adjuvant SRT on the resected area. In a single center study, the volume of the lesions was correlated with greater local recurrence and central necrosis rates after SRT or WBRT [42]. Even so, they also clarified that this was not the case when SRT and WBRT were preceded by local surgical resection [42].

 doi:10.20944/preprints202602.1448.v1

The superiority of the protocol resides in the fact that it is more effective to irradiate the remaining postoperative area than the entire lesion; with a lesser total volume to irradiated and thus greater allowed doses that consequently lower the rate of local recurrence. This protocol could also be useful in better SRT control over previously surgically depleted cystic lesions [4].

The inclusion of patients with more than 5 lesions in SRT protocols is yet to be decided, nevertheless numerous studies found that patients with 5 to 10 BMs, or in some cases even more than 10, could benefit from radiotherapy with improved OS [43][44].

4.2. ML Models Results' Implications

Using the same four models for three different situations enabled us to compare them not only by specific metrics but also depending on the data that was submitted.

When both sets of data, containing clinical and treatment protocol information, together with MRI features were evaluated, every model had a better performance status than in analyzing the two sets of data separately.

The analysis of only clinical data obtained the worst outcomes and the models were the least performant in OS prediction, the best one being RF (see Figure B1 in Appendix B).

The assessment of only MRI features along with treatment protocols allowed the models to achieve better results, but still not competitive enough (see Figure B2 in Appendix B)

The addition of MRI features to the clinical ones has proven to boost the prediction of OS by the ML models, with greater metrics values and better discrimination (see Figure B3 in Appendix B). In this case, NN was the model that obtained the greater prediction values and discriminatory power (AUC=0.93).

Regarding feature importance, the SHAP analysis easily identified the more relevant ones and their clinical implication in OS (see Figure 4).

The clinical features that were selected are number of lesions and presence of systemic metastases, in correlation with the survival analysis. These two factors are already part of different prognostic appreciation and risk stratification scales [3]. Synchronism was also selected with poor prognostic value. In some studies, synchronic diagnosis is younger patients is correlated with longer survival compared to metachronous diagnosis in patients over 65 years of age [1].

Other clinical characteristics did not reach significance: age, sex, diabetes or smoker status. Also, the presence of leptomeningeal involvement did not affect survival, in contradiction with other findings, as leptomeningeal metastases are known to be an independent poor prognosis factor in OS [45][46].

As a result of the partly retrospective nature of the study, missing data is one weakness of this kind of research and the Karnovsky score was missing data. Its prognostic value has long been demonstrated by numerous studies and it is currently used, alone or in prognostic scales for the stratification of the patients' risk and the determination of the treatment option.

There are however studies which did not find a correlation between the GPA score and OS [14]. Other studies found that GPA had a limited precision of prognostic estimation, of only 3-6 months [11]. Considering that the OS of metastatic patients is getting longer because of the improvement of treatment protocols [47], new and more comprehensive prognostic scores should be developed in order to be used on a longer period of time.

Of the different protocols, GK and WBRT have been selected as protective factors by both the survival analysis and the prediction model NN, with GK being associated with longer survival. This conclusion is in accordance with other studies on OS [48].

The MRI features that obtained importance are: volume of lesions, contrast intake type (solid with/ without central necrosis versus cystic and mixt), vascularization, hemorrhage and restricted diffusion.

Recent studies consider total volume of BMs is more important in OS prediction than number of lesions [41]. In the case of SRT, for example, the total volume of the lesions can be more relevant than the number because the allowed irradiation dose is inversely related to the total volume of the lesions [2][7]. Other studies found the median volume and size of the lesions as an important prognostic factor in BMs from different primary tumors [49] [31].

 doi:10.20944/preprints202602.1448.v1

The NN and RF models sustained the survival analysis findings in which restricted diffusion is associated with poor prognosis. Other studies comparing different types of BMs found that restricted diffusion can differentiate SCLC metastases from NSCLC, as SCLC showed greater cellularity and worse prognosis, despite being more radiosensitive [50][51].

All the models found that the presence of a cystic component in the cystic and mixt types of BMs was associated with poor prognosis comparative to solid lesions [2].

The presence of internal vascularization was also found to be of importance, having a negative impact on OS by the NN and RF models. Contrary to vascularization, the presence of microhemorrhages was found to be positively correlated with survival by the NN model. This finding is in contradiction with general knowledge regarding internal tumoral bleeding, that is often correlated to hemorrhagic BMs with poor prognosis (melanoma) [1].

Possible reasons for such results are previously explained. Additionally, because metastatic MRI features are less explored comparative to primary brain tumors, there is insufficient data to have pertinent conclusions and also a limited number of studies to compare our results with. Thus, the need to further explore how internal hemorrhage and blood-brain barrier integrity could affect local treatment outcomes, remains of great importance.

All the ML algorithms performed better when MRI features were added to clinical and treatment data, in predicting OS at 6 months. These findings, once again emphasize on the need of developing models that include morphological MRI characteristics of BMs that can further contribute to clinical decision making.

4.2. Limitations

Because all the patients included in this study were admitted at diagnosis in a neurosurgery hospital, all of them had different neurological symptoms. This can be viewed as a selection bias, as no asymptomatic patients were included in the study. Likewise, the fact that we included only histologically confirmed patients can also be seen as a selection bias, as multiple patients were excluded from our study; however, this was a critical step in order to ensure the quality of our data and also the possibility to evaluate the prognostic value of the nature of the primary tumor.

The Karnovsky score was not included in our study as a prognostic factor because it was missing data.

Although the quality of the data is satisfactory, the number of patients and secondary lesions could also poorly affect the ML models, as they are known to operate on more sustainable data.

To minimize overfitting, we carefully selected the features implemented, as feature selection is the first step in ensuring a model's clarity. We also implemented a recursive feature elimination with grid search cross-validation to find the best feature combination and hyperparameters for each model, with feature scaling. The temporal validation of the four models is another limitation of the study, as external validation is usually superior.

5. Conclusions

Our results confirm that including morphological MRI features of BMs in the prediction of OS significantly contributes to the enhancement of ML algorithms prediction and discriminatory capacity.

Of the significant variables, a high number of BMs, greater volumes, restricted diffusion, internal vascularization, the presence of a cystic component, extracranial metastasis and synchronism are found to be poor prognostic factors; on the other hand, lesser volume, single lesions, solid enhancement and radiotherapy were found to be good prognostic factors. The best treatment protocol is yet to be decided, our results suggest that surgery followed by SRT is the best choice for single lesions or oligometastatic disease.

This study could contribute in predefine important MRI metastatic features in future research regarding survival and prognostic appreciation, with the aim to include novel MRI prognostic factors in clinical practice to ensure a personalized approach in BMs management.

 doi:10.20944/preprints202602.1448.v1

Author Contributions: Conceptualization, D.P., M.P.R. and O.M.O.; methodology, C.C., D.P., O.M.O; software, O.M.O.; formal analysis, D.P., O.M.O.; investigation, D.P., E.A.M., S.I.C.; resources, D.P., C.C., B.I.D., M.R.P.; data curation, D.P., C.C., E.A.M.; writing—original draft preparation, D.P., S.I.C; writing—review and editing, C.C., D.P., S.I.C.; visualization, B.I.D., M.P.R., D.H.; supervision, D.H., E.A.M.; project administration, D.P., D.H., B.I.D. All authors have read and agreed to the published version of the manuscript.

Funding: This research received no external funding.

Institutional Review Board Statement: The study was conducted in accordance with the Declaration of Helsinki and approved by the Ethics Committee of both the University of Medicine and Pharmacy "Grigore T. Popa" (Nr. 422/02.04.2024) and the Clinical Emergency Hospital "Prof. Dr. Nicolae Oblu" (Nr. 10/08.11.2023) from which the cases were obtained.

Informed Consent Statement: Patient consent was waived due to the retrospective nature of the study.

Data Availability Statement: Our data is not publicly available due to ethical restrictions, but can be accessed through the corresponding authors on reasonable request.

Acknowledgments: We would like to express our gratitude to the radiology technicians and histopathology department of the Clinical Emergency Hospital "Prof. Dr. Nicolae Oblu".

Conflicts of Interest: The authors declare no conflicts of interest.

Abbreviations

The following abbreviations are used in this manuscript:

BM(s)	Brain Metastasis
OS	Overall Survival
WBRT	Whole Brain Radiotherapy
SRS	Stereotactic Radio-Surgery
SRT	Fractionated Radiotherapy
CHT	Chemotherapy
MRI	Magnetic Resonance Imaging
T1W	T1-wheigthed
T2W	T2-wheighted
T2W FLAIR	T2-wheighted Fluid Attenuated Inversion Recovery
GPA	Graded Prognostic Assessment
DS-GPA	Disease Specific GPA
RANO	Response Assessment in Neuro-Oncology
RECIST	Response Evaluation Criteria in Solid Tumors
AI	Artificial Intelligence
SWI	Susceptibility Weighted Imaging
DWI	Diffusion-weighted Imaging
ADC	Apparent Diffusion Coefficient
CE T1W	Contrast-enhanced T1-wheigthed
BSC	Best Supportive Care
GK	Gamma-knife
EDA	Explanatory Data Analysis
KM	Kaplan-Meier
HR	Hazard Ratio
CI	Intervals Of Confidence
ML	Machine Learning
XGBoost	Extreme Gradient Boosting
NN	Neural Network
KNN	K-Nearest Neighbor
RF	Random Forest
ROC	Receiver Operating Characteristics
AUC	Aria Under the ROC Curve

 doi:10.20944/preprints202602.1448.v1

SHAP Shapley Additive Explanations

Appendix A

The MRI acquisition parameters differ for every sequence (see Table A1), the echo number is equal to 1, and the matrix is 256/256 for DWI/ADC and 512/512 for the other sequences.

Table A1. Parameter acquisition for every MRI sequence.

Sequence	Slice thickness (mm)	Spacing (mm)	TE* (s)	TR** (s)
T1W	1.8-2	0.8-1	3.5-4.2	8-9.6
T2W	4-5	5	104-110	4101-6215
T2W FLAIR	1.2-1.8	0.6-0.8	119-300	4800-7002
DWI	4-5	4-6	83.59-84.5	4600-8201
ADC	4-5	4-6	83.59-84.5	4600-8201
SWI	3	1-1.5	~49	52-79
CE T1W	1-1.8	0.8-1	3.5-4.2	8-9.2

* Time to echo; ** Repetition time. .

The characteristics of our dataset is visible in Table A2, where we can find the age at diagnosis, sex, nature of primary tumor, synchronism, number of lesions and other comorbidities. Note that age at diagnosis was further analyzed as numerical data in Table A3.

Table A2. Patients' characteristics and survival time in months (EDA).

Characteristic	Number/ Type	Mean time	SD*	Min	25%	50% (median)	75%	Max
Age at diagnosis	**> 65 y.o. (41 – 59.6%)**	9.86	10.04	0.46	3.53	6.46	12.83	50.9
	< 65 y.o. (68 – 62.4%)	11.26	10.36	0.5	3.99	8.8	15.56	52.1
Sex	M (71 – 65.1%)	10.12	10.76	0.46	3.1	6.7	13.06	52.1
	F (38 – 34.9%)	11.83	9.15	0.5	4.18	11.31	17.39	35.53
Primary tumor	NSCLC (55 – 50.46%)	11.10	10.22	0.46	4.46	8.1	14.38	50.9
	SCLC (7 – 6.43%)	6.24	6.39	0.6	0.88	3.73	11.01	15.56
	Breast (14 – 12.84%)	16.21	11.02	0.96	7.91	14.11	22.57	35.53
	Digestive (7 – 6.43%)	8.26	5.91	1.43	4.31	7	11.1	18.6
	Melanoma (12 – 11%)	6.54	7.26	1.36	1.88	4.58	7	27.6
	Other (10 – 9.17%)	12.63	14.88	1.83	4.21	6.71	14.06	52.1
	Unknown (4 – 3.67%)	6.69	5.66	0.5	2.87	6.58	10.4	13.1
Synchronous	63 (57.8%)	8.45	8.38	0.5	3.31	6.2	10.41	52.1
Metachronous	46 (42.2%)	13.87	11.67	0.46	4.23	12.43	20.05	50.9
Number of metastases	Single (54 – 49.54%)	12.77	11.7	0.46	4.6	8.8	18.45	52.1

 doi:10.20944/preprints202602.1448.v1

	Multiple (55 – 50.46%)	8.75	8.14	0.5	3.1	6.46	12.48	45.16
LM**	Yes (31 – 28.44%)	11.07	11.45	0.46	2.51	7.9	14.3	52.1
	No (78 - 71.56%)	10.6	9.76	0.83	3.77	7.53	14.01	50.9
Extracranial metastases	Yes (42 – 38.53%)	9.2	7.29	0.5	3.25	7.43	12.96	35.1
	No (67 – 61.47%)	12	11.67	0.46	4.1	8.03	15.56	52.1
Diabetes	Yes (17 – 15.6%)	8.91	8.85	0.93	3.53	7	10.66	35.53
	No (92 – 84.4%)	11.07	10.46	0.46	3.65	8.08	14.9	52.1
Smoker status (declaratively)	Smoker (13 – 12%)	10.9	11.18	0.60	5.13	9.7	13.03	45.16
	Non-smoker (96 – 88%)	10.72	10.14	0.46	3.42	7.05	14.9	52.1
Complications	Yes (29 – 26.6%)	10.73	11.66	0.46	3.03	5.26	14.76	50.9
	No (80 – 73.4%)	10.74	9.72	0.5	3.95	8	14	52.1

*Standard deviation, ** Leptomeningeal metastasis.

Table A3. Patients' age (numerical values) and survival time in months (EDA).

Age at diagnosis	Number	Mean time	SD*	Min	25%	50%	75%	Max
<40	5 (4.6%)	13.52	10.26	1.5	6.56	12.93	19.03	27.6
40-50	12 (11%)	8.83	6.47	1.43	3.74	8.78	12.39	21
50-60	29 (26.5%)	11.82	11.52	0.5	3.1	10.36	17.86	52.1
60-70	52 (48%)	10.98	10.81	0.46	3.65	7.5	13.35	50.9
70-80	10 (9%)	8.24	6.84	0.86	4.35	6.73	9.85	23.4
>80	1 (0.9%)	0.6	-	0.6	0.6	0.6	0.6	0.6

*Standard deviation, ** Leptomeningeal metastasis.

For the MRI features of secondary lesions, an EDA was also performed, visible in Table A4. In this case survival was appreciated taking into regard imaging characteristics of every secondary lesion for every patient.

Table A4. MRI features analyzed for every BM and survival in months (EDA).

MRI features	Number/ Type	Mean time	SD*	Min	25%	50%	75%	Max
Internal vascularization	Yes (94 – 25.4%)	9.27	8.68	0.83	2.68	7.05	13.1	52.1
	No (276 – 74.6%)	7.95	8.19	0.46	0.86	5.86	12.39	50.9
Internal hemorrhage	Yes (68 – 18.38%)	11.56	10.81	0.6	4.27	9.7	14.76	52.1
	No (302 – 81.62%)	7.55	7.48	0.46	0.86	5.76	12.3	45.16

 doi:10.20944/preprints202602.1448.v1

Contrast intake type	Solid (107 – 28.9%)	9.44	7.54	0.5	4.03	10.1	12.66	45.16
	Solid with necrosis (138 – 37.3%)	10.08	7.97	0.5	3.83	8.08	12.98	45.16
	Cystic (93 – 25.2%)	3.91	7.55	0.83	0.83	0.83	1.1	50.9
	Mixt (32 – 8.6%)	9.43	10.16	0.46	2.44	6.78	12.77	52.1
Edema	Yes (209 – 56.48%)	10.27	9.56	0.46	3.03	7.96	14.13	52.1
	No (161 – 43.52%)	5.72	5.41	0.5	0.83	4.03	10.36	22.96
Diffusion restriction	Yes (191 – 51.62%)	6.70	8.67	0.46	0.83	3.1	9.9	52.1
	No (179 – 48.38%)	9.98	7.61	0.5	4.03	10.1	12.66	45.16
Greater diameter	< 5 mm (268 – 72.5%)	7.67	7.74	0.5	0.86	5.86	12.3	45.16
	Between 5 and 10 mm (24 – 6.5%)	9.65	7.26	0.6	3.51	7.11	14.96	23.96
	>10 mm (78 – 21%)	9.99	10.18	0.46	3.05	6.98	13.08	52.1
Site	Supratentorial (275 – 74.3%)	8.47	8.63	0.46	0.93	6.46	12.66	52.1
	Infratentorial (95 – 25.7%)	7.77	7.41	0.5	1.83	5.53	10.96	35.53

* Standard deviation.

Because the volume of the BMs turns out to be very important in OS estimation, the following tables, Table A5 and A6 contain supplementary information about relations between size (diameter and volume) and number of secondary lesions.

Table A5. Diameters (mm) and volumes (cm³) of BMs (EDA).

Greater diameter of BMs (mm)	BMs	Mean volume	SD*	Min volume	25%	50%	75%	Max volume
<5	268 (72.5%)	0.75	1.08	0.03	0.05	0.2	0.9	4.92
>=5 and <10	24 (6.5%)	7.23	1.61	5.04	5.61	6.82	8.74	9.4
>=10	78 (21%)	31.7	21.55	10.13	16.9	26.03	37.01	121.23

* Standard deviation.

Table A6. Total number of BMs per patient and volumes (cm³) of BMs (EDA).

Total number of BMs	Patients	Mean volume	SD*	Min volume	25%	50%	75%	Max volume
1	54 (49.5%)	27.66	25.89	1.67	8.78	19.47	36.99	121.23
1-5	42 (38.5%)	6.9	5.91	0.03	1.77	5.87	10.85	25.58
>5	13 (12%)	3.43	2.12	0.70	1.91	3.42	5.13	7.65

* Standard deviation.

The last table in this Appendix is dedicated to treatment protocols used in our cohort and their implication in OS. Table A7 delivers an overview of treatment choice over survival.

 doi:10.20944/preprints202602.1448.v1

Table A7. Treatment options and their OS (months).

Treatment	Number/ Type	Mean time	SD*	Min	25%	50%	75%	Max
Chemotherapy	Yes (13 – 12%)	18.65	14.03	4.63	6.96	12.3	24.43	50.9
	No (96 – 88%)	9.67	9.11	0.46	3.09	6.85	13.24	52.1
Surgery	Yes (99 - 90.8%)	11.27	10.47	0.46	3.88	8.06	15.03	52.1
	No (10 – 9.1%)	5.42	4.86	0.6	1.21	4.3	7.66	13.96
SRT (GK)	Yes (22 – 20.2%)	14.44	10.9	1.36	9.65	12.53	15.96	50.9
	No (87 – 79.8%)	9.8	9.88	0.46	3.05	6.26	13.35	52.1
WBRT	Yes (9 – 8.3%)	19.45	14.69	4.1	12.06	13.1	21.4	50.9
	No (100 – 91.7%)	9.95	9.43	0.46	3.1	6.83	13.74	51.1

* Standard deviation.

Appendix B

In this Appendix we included two heatmaps representing the metric of the ML models used in the appreciation of prognosis at 6 months for BMs patients, in the case of only using clinical data (Figure B1), in the case of using only morphological MRI data (Figure B2) and both sets of data (Figure B3).

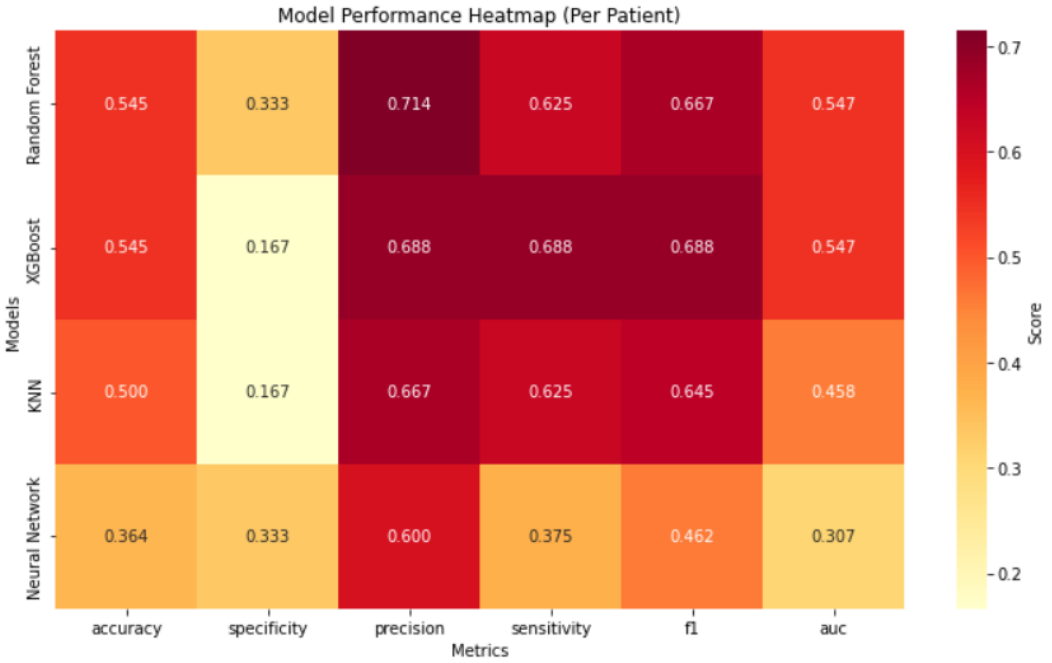

Figure B1. Heatmap showing prediction performance using only clinical data.

 doi:10.20944/preprints202602.1448.v1

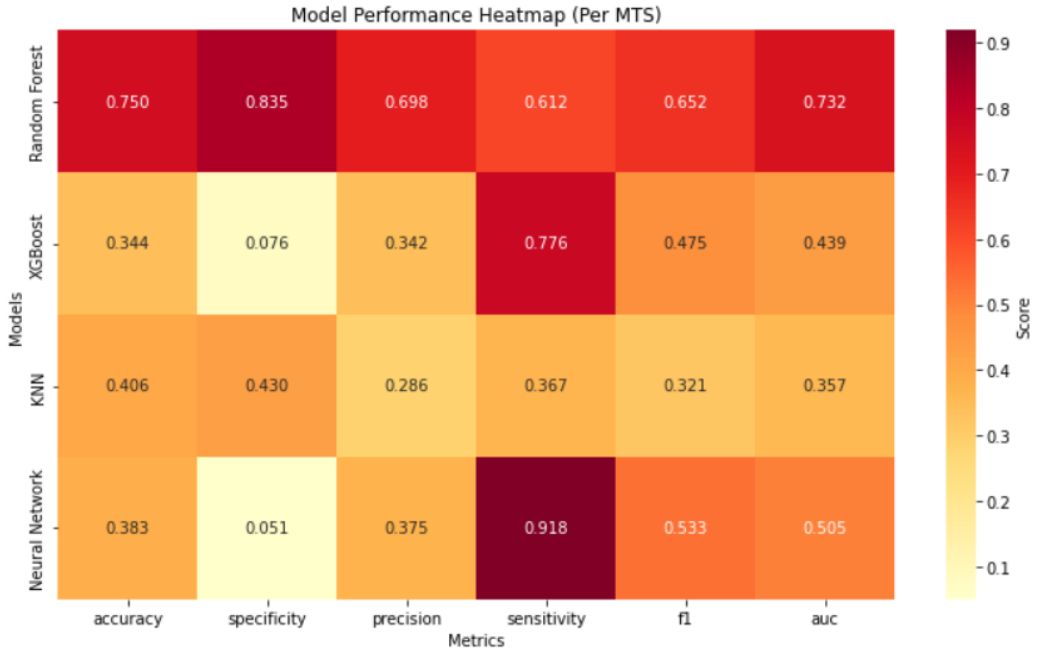

Figure B2. Heatmap showing prediction performance using only MRI morphological data.

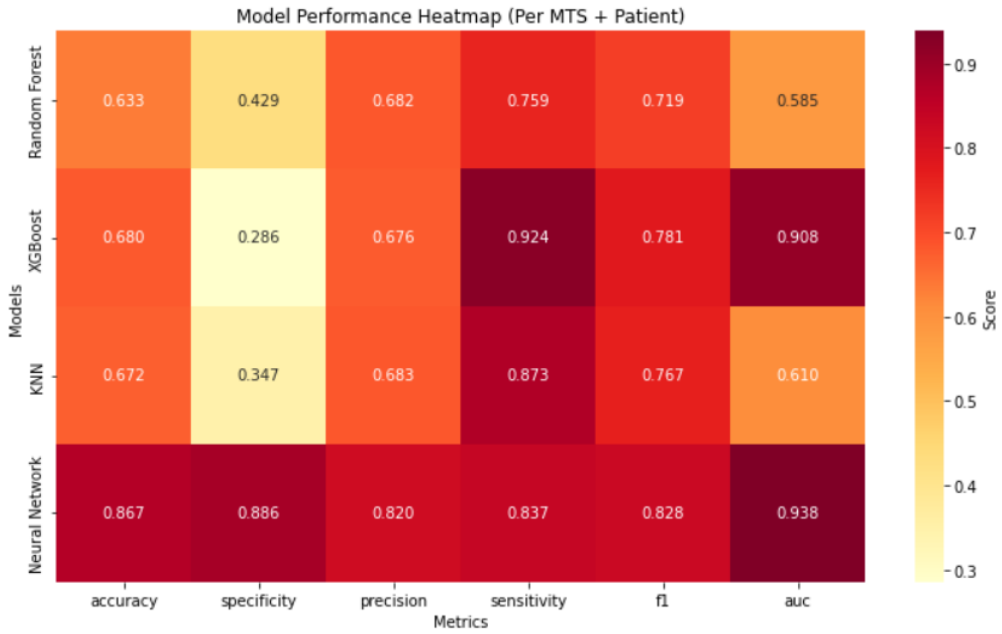

Figure B3. Heatmap showing prediction performance using only MRI morphological dat.

References

1. Lamba N, Wen PY, Aizer AA. Epidemiology of brain metastases and leptomeningeal disease. Vol. 23, Neuro-Oncology. Oxford University Press; 2021. p. 1447–56; DOI=10.1093/neuonc/noab101.
2. Pellerino A, Rudà R, Soffietti R. Brain Metastases including those for text and data mining, AI training, and similar technologies. 2024; Available from: https://doi.org/10.1016/B978-0-323-95702-1.00198-6; DOI=10.1016/B978-0-323-95702-1.00198-6.
3. Aizer AA, Lamba N, Ahluwalia MS, Aldape K, Boire A, Brastianos PK, et al. Brain metastases: A Society for Neuro-Oncology (SNO) consensus review on current management and future directions. Neuro Oncol. 2022 Oct 1;24(10):1613–46; DOI=10.1093/neuonc/noac118.

 doi:10.20944/preprints202602.1448.v1

4. Le Rhun E, Guckenberger M, Smits M, Dummer R, Bachelot T, Sahm F, et al. EANO–ESMO Clinical Practice Guidelines for diagnosis, treatment and follow-up of patients with brain metastasis from solid tumours ☆. Annals of Oncology. 2021 Nov 1;32(11):1332–47; DOI=10.1016/j.annonc.2021.07.016.
5. Burt Nabors L, Portnow J, Baehring J, Bhatia A, Bloch O, Brem S, et al. NCCN Guidelines Version 1.2025 Central Nervous System Cancers Continue NCCN Guidelines Panel Disclosures [Internet]. 2025. Available from: https://www.nccn.org/home/member.
6. Gupta S, Singh S, Chophy A, Nair S, Ahuja R, Kusum K, et al. Analysis of prognostic factors in patients with brain metastases affecting survival. J Egypt Natl Canc Inst. 2022 Dec 1;34(1); DOI=10.1186/s43046-022-00146-z.
7. Kretzschmar L, Gabrys H, Joye A, Kraft J, Guckenberger M, Andratschke N. Postoperative stereotactic radiosurgery (SRS) vs hypofractionated stereotactic radiotherapy (SRT) for resected brain metastases – a single centre analysis. Clin Exp Metastasis. 2025 Apr 1;42(2) ; DOI=10.1007/s10585-025-10334-5.
8. Lu Y, Huang Y, Zhu C, Li Z, Zhang B, Sheng H, et al. Cancer brain metastasis: molecular mechanisms and therapeutic strategies. Vol. 6, Molecular Biomedicine. Springer Nature; 2025; DOI=10.1186/s43556-025-00251-0.
9. Kaufmann TJ, Smits M, Boxerman J, Huang R, Barboriak DP, Weller M, et al. Consensus recommendations for a standardized brain tumor imaging protocol for clinical trials in brain metastases. Vol. 22, Neuro-Oncology. Oxford University Press; 2020. p. 757–72; DOI=10.1093/neuonc/noaa030.
10. Sperduto PW, Kased N, Roberge D, Xu Z, Shanley R, Luo X, et al. Summary report on the graded prognostic assessment: An accurate and facile diagnosis-specific tool to estimate survival for patients with brain metastases. Journal of Clinical Oncology. 2012 Feb 1;30(4):419–25; DOI= 10.1200/JCO.2011.38.0527.
11. Villà S, Weber DC, Moretones C, Mañes A, Combescure C, Jové J, et al. Validation of the new graded prognostic assessment scale for brain metastases: A multicenter prospective study. Radiation Oncology. 2011 Mar 2;6(1); DOI=10.1186/1748-717X-6-23.
12. Ribeiro LM, Bomtempo FF, Rocha RB, Telles JPM, Neto EB, Figueiredo EG. Development and adaptations of the Graded Prognostic Assessment (GPA) scale: a systematic review. Vol. 40, Clinical and Experimental Metastasis. Springer Science and Business Media B.V.; 2023. p. 445–63; DOI=10.1007/s10585-023-10237-3.
13. Erich Yri O, Lindviksmoen Astrup G, Telhaug Karlsson A, van Helvoirt R, Jensen Hjermstad M, Moksnes Husby K, et al. Survival and quality of life after first-time diagnosis of brain metastases: a multicenter, prospective, observational study [Internet]. 2024. Available from: www.thelancet.com; DOI=10.1016/j.lanepe.2024.101181.
14. Ocaña-Tienda B, Pérez-Beteta J, Ortiz de Mendivil A, Asenjo B, Albillo D, Pérez-Romasanta LA, et al. Morphological MRI features as prognostic indicators in brain metastases. Cancer Imaging. 2024 Dec 1;24(1); DOI=10.1186/s40644-024-00753-0.
15. Chukwueke UN, Wen PY. Use of the Response Assessment in Neuro-Oncology (RANO) criteria in clinical trials and clinical practice. Vol. 8, CNS Oncology. Newlands Press Ltd; 2019; DOI=10.2217/cns-2018-0007.
16. Khalighi S, Reddy K, Midya A, Pandav KB, Madabhushi A, Abedalthagafi M. Artificial intelligence in neuro-oncology: advances and challenges in brain tumor diagnosis, prognosis, and precision treatment. Vol. 8, Precision Oncology. Nature Research; 2024; DOI=10.1038/s41698-024-00575-0.
17. Wichmann JL, Willemink MJ, De Cecco CN. Artificial Intelligence and Machine Learning in Radiology: Current State and Considerations for Routine Clinical Implementation. Vol. 55, Investigative Radiology. Lippincott Williams and Wilkins; 2020. p. 619–27; DOI=10.1097/RLI.0000000000000673.
18. Grover VPB, Tognarelli JM, Crossey MME, Cox IJ, Taylor-Robinson SD, McPhail MJW. Magnetic Resonance Imaging: Principles and Techniques: Lessons for Clinicians. Vol. 5, Journal of Clinical and Experimental Hepatology. Elsevier B.V.; 2015. p. 246–55 ; DOI= 10.1016/j.jceh.2015.08.001.
19. Le Fèvre C, Sun R, Cebula H, Thiery A, Antoni D, Schott R, et al. Ellipsoid calculations versus manual tumor delineations for glioblastoma tumor volume evaluation. Sci Rep. 2022 Dec 1;12(1) ; DOI= 10.1038/s41598-022-13739-4.
20. Lin NU, Lee EQ, Aoyama H, Barani IJ, Barboriak DP, Baumert BG, et al. Response assessment criteria for brain metastases: Proposal from the RANO group. Vol. 16, The Lancet Oncology. Lancet Publishing Group; 2015. p. e270–8; DOI= 10.1016/S1470-2045(15)70057-4.

 doi:10.20944/preprints202602.1448.v1

21. Komorowski M, Marshall DC, Salciccioli JD, Crutain Y. Exploratory Data Analysis, In: Secondary Analysis of Electronic Health Records. Springer International Publishing; 2016. p. 185-203; DOI=10.1007/978-3-319-43742-2_15.
22. Kaplan EL, Meier P. Nonparametric Estimation from Incomplete Observations*, In Breakthroughs in Statistics. Springer-Verlag New York; 1992. P. 320-337.
23. Woolson RF. Rank Tests and a One-Sample Logrank Test for Comparing Observed Survival Data to a Standard Population [Internet]. Vol. 37. Biometrics. International Biometric Society; 1981. p. 687-696 Available from: http://www.jstor.org.
24. Abd Elhafeez S, D'Arrigo G, Leonardis D, Fusaro M, Tripepi G, Roumeliotis S. Methods to Analyze Time-to-Event Data: The Cox Regression Analysis. Oxid Med Cell Longev. 2021; DOI= 10.1155/2021/1302811.
25. Ramspek CL, Jager KJ, Dekker FW, Zoccali C, Van DIepen M. External validation of prognostic models: What, why, how, when and where? Vol. 14, Clinical Kidney Journal. Oxford University Press; 2021. p. 49–58; DOI= 10.1093/ckj/sfaa188.
26. Chen T, Guestrin C. XGBoost: A scalable tree boosting system. In: Proceedings of the ACM SIGKDD International Conference on Knowledge Discovery and Data Mining. Association for Computing Machinery; 2016. p. 785–94; DOI= 10.1145/2939672.2939785.
27. Chaki J, Ucar A. Current Applications of Deep Learning in Cancer Diagnostics. CRC Press; 2023; DOI= 10.1201/9781003277002.
28. Mendelson EB. Artificial intelligence in breast imaging: Potentials and limitations. Vol. 212, American Journal of Roentgenology. American Roentgen Ray Society; 2019. p. 293–9; DOI= 10.2214/AJR.18.20532.
29. Brause RW, Goethe JW. Medical Analysis and Diagnosis by Neural Networks. Vol. 2199, LNCS. Springer-Verlag; 2001; DOI= 10.1007/3-540-45497-7_1.
30. Guo G, Wang H, Bell D, Bi Y, Greer K. LNCS 2888 - KNN Model-Based Approach in Classification. Vol. 2888, LNCS. 2003; DOI= 10.1007/978-3-540-39964-3_62.
31. Öznacar T, Aral İP, Zengin HY, Tezcan Y. Survival Prediction in Brain Metastasis Patients Treated with Stereotactic Radiosurgery: A Hybrid Machine Learning Approach. Brain Sci. 2025 Mar 1;15(3); 10.3390/brainsci15030266.
32. Breiman L. Random Forests. Vol. 45, Machine Learning; 2001. p. 5-32; DOI= 10.1023/A:1010933404324.
33. Baratloo A, Hosseini M, Negida A, El Ashal G. Part 1: Simple Definition and Calculation of Accuracy, Sensitivity and Specificity. Emerg (Tehran). 2015 Spring;3(2):48-9. PMID: 26495380; PMCID: PMC4614595.
34. Noman SM, Fadel YM, Henedak MT, Attia NA, Essam M, Elmaasarawii S, et al. Leveraging survival analysis and machine learning for accurate prediction of breast cancer recurrence and metastasis. Sci Rep. 2025 Dec 1;15(1):3728; DOI= 10.1038/s41598-025-87622-3.
35. Lundberg S, Lee SI. A Unified Approach to Interpreting Model Predictions. 2017 May 22; Available from: http://arxiv.org/abs/1705.07874; DOI= 10.48550.
36. Potthoff AL, Heimann M, Lehmann F, Ilic I, Paech D, Borger V, et al. Survival after resection of brain metastasis: impact of synchronous versus metachronous metastatic disease. J Neurooncol. 2023 Feb 1;161(3):539–45; DOI= 10.1007/s11060-023-04242-5.
37. Teng YC, Chen J, Zhong WB, Liu YH. Construct a Refined Monte Carlo Model for BNCT Dose Calculation and Assessment by Converting HU Value to Material Compositions for ROIs [Internet]. 2024. Available from: https://www.researchsquare.com/article/rs-4492683/v1; DOI= 10.21203/rs.3.rs-4492683/v1.
38. Skogen K, Schulz A, Helseth E, Ganeshan B, Dormagen JB, Server A. Texture analysis on diffusion tensor imaging: discriminating glioblastoma from single brain metastasis. Acta radiol. 2019 Mar 1;60(3):356–66 ; DOI= 10.1177/0284185118780889.
39. Qin X, Liu R, Akter F, Qin L, Xie Q, Li Y, et al. Peri-tumoral brain edema associated with glioblastoma correlates with tumor recurrence. J Cancer. 2021 Feb 5;12(7):2073–82; DOI= 10.7150/jca.53198.
40. Kim MS, Park SH, Park ES, Park JB, Kwon SC, Lyo IU, et al. Quantitative analysis in peritumoral volumes of brain metastases treated with stereotactic radiotherapy. Journal of Neuroradiology. 2018 Sep 1;45(5):310–5; DOI= 10.1016/j.neurad.2017.12.022.

 doi:10.20944/preprints202602.1448.v1

41. Bhattacharya K, Mahajan A, Mynalli S. Imaging Recommendations for Diagnosis, Staging, and Management of Central Nervous System Neoplasms in Adults: CNS Metastases. Vol. 16, Cancers. Multidisciplinary Digital Publishing Institute (MDPI); 2024; DOI= 10.3390/cancers16152667.
42. Rashid NS, Lamba N, Catalano PJ, Elhalawani H, Tanguturi SK, Rahman R, et al. Impact of brain metastasis size at the time of radiotherapy on local control and radiation necrosis. J Neurooncol. 2025 ; DOI= 10.1007/s11060-025-05023-y.
43. Kotecha R, La Rosa A, Brown PD, Vogelbaum MA, Navarria P, Bodensohn R, et al. Multidisciplinary management strategies for recurrent brain metastasis after prior radiotherapy: An overview. Neuro Oncol. 2025 Mar 1;27(3):597–615 ; DOI= 10.1093/neuonc/noae220.
44. Susko MS, Garcia MA, Ma L, Nakamura JL, Raleigh DR, Fogh S, et al. Stereotactic Radiosurgery to More Than 10 Brain Metastases: Evidence to Support the Role of Radiosurgery for Ideal Hippocampal Sparing in the Treatment of Multiple Brain Metastases. World Neurosurg. 2020 Mar 1;135:e174–80; DOI= 10.1016/j.wneu.2019.11.089.
45. Lee GH, Seol YM, Choi YJ, Kim H. Prognostic factors of brain metastasis and subsequent survival in breast cancer patients: An 11-year, single-center, retrospective study. Medicine (United States). 2025 Mar 14;104(11):e41827; DOI= 10.1097/MD.0000000000041827.
46. Le Rhun E, Devos P, Weller J, Seystahl K, Mo F, Compter A, et al. Prognostic validation and clinical implications of the EANO ESMO classification of leptomeningeal metastasis from solid tumors. Neuro Oncol. 2021 Jul 1;23(7):1100–12; DOI= 10.1093/neuonc/noaa298.
47. Cooke CM, Babadagli ME, Wilson H, Nair VJ, Lupe K, Malone S, et al. Brain Metastases in Gynaecologic Cancer: A Retrospective Cohort Study Evaluating Treatment Outcomes, Prognostic Factors, and Overall Survival. Current Oncology. 2024 Dec 1;31(12):7575–85; DOI= 10.3390/curroncol31120558.
48. Sander C, Frydrychowicz C, Prasse G, Taubenheim S, Arlt F, Meixensberger J, et al. The impact of neurological performance and volumetrics on overall survival in brain metastasis in colorectal cancer: a retrospective single-center case series. BMC Cancer. 2022 Dec 1;22(1); DOI= 10.1186/s12885-022-09435-1.
49. Kanakarajan H, De Baene W, Gehring K, Eekers DBP, Hanssens P, Sitskoorn M. Factors associated with the local control of brain metastases: a systematic search and machine learning application. Vol. 24, BMC Medical Informatics and Decision Making. BioMed Central Ltd; 2024; DOI= 10.1186/s12911-024-02579-z.
50. Zhu D, Shao Y, Yang Z, Cheng A, Xi Q, Liang X, et al. Magnetic resonance imaging characteristics of brain metastases in small cell lung cancer. Cancer Med. 2023 Jul 1;12(14):15199–206; DOI= 10.1002/cam4.6206.
51. Incesu L, Abdullayev S, Ozturk M, Aslan K, Gunbey HP. Role of apparent diffusion coefficient measurement in differentiating histological subtypes of brain metastasis of lung cancer. Rev Assoc Med Bras. 2022;68(9):1318–23; DOI= 10.1590/1806-9282.20220630.